Supporting Information for the Manuscript Entitled

Effect of release of dopamine on iron transformations and reactive oxygen species (ROS) generation under conditions typical of coastal waters

School of Civil and Environmental Engineering, The University of New South Wales, Sydney, NSW 2052, Australia

Keywords: quinones, ROS, iron stress, dopamine, melanin and macroalgae

Environmental Sciences: Processes and Impacts

December, 2017

* Corresponding author. Professor T. David Waite, Tel.: +61 2 9385 5059, Email: d.waite@unsw.edu.au

SI 1 Materials and Methods

All analytical grade chemicals were purchased from Sigma-Aldrich (or as otherwise stated) and were used without further refinement. All solutions were prepared using 18 MΩ.cm ultrapure Milli-Q water (MQ). All glassware was acid washed in 5% v/v HCl for at least one week before use. Stock solutions were kept in dark bottles and were refrigerated at 4 ^{o}C when not in use. All pH measurements were conducted using a Hanna HI9025 pH meter combined with a glass electrode and Ag/AgCl reference. Calibration of the pH electrode was undertaken using NIST buffer solutions (pH 7.01 and 10.01). Experiments were conducted in darkness with the reactor covered in foil for the duration of the reaction.

A concentrated Fe(II) stock solution (5 mM) was prepared by dissolving ferrous ammonium sulfate hexahydrate ($Fe(NH_4SO_4)_2 \cdot 6H_2O$) in 10 mM HCl. Concentrated stock solutions of 10 mM Fe(III) (using ferric chloride hexahydrate ($FeCl_3 \cdot 6H_2O$) and 10 mM DA were prepared weekly in 10 mM HCl. The working stock solutions of Fe(II), Fe(III) and DA were diluted from the concentrated stock solutions daily in 10 mM HCl solution. The acidity of both concentrated stock and working stock solutions was sufficient to avoid significant oxidation of Fe(II) and DA and precipitation of Fe(III) on the time scale of interest and yet low enough to minimize any pH change that might occur on addition of the stock to experimental solutions. A stock solution of 20 mM H_2O_2 prepared by dilution of a nominal 30% w⁄w H_2O_2 solution was used for calibration of the H_2O_2 measurements. The nominal 30% w⁄w solution was standardized by UV spectrophotometry at 240 nm. [1] Concentrated stock solutions of 80 mM ferrozine (FZ) and 20 mM desferrioxamine B (DFB) were prepared in MQ. A daily prepared mixture containing 50 mM FZ and 5 mM DFB was used for Fe(II) determination. Stock solutions of 60 mM N,N-diethyl-p-phenylenediamine (DPD) and 500 KU/L horseradish peroxidase (HRP) were prepared in MQ water as described previously. [2] A 10 mM stock solution of diethylenetriaminepentaacetic acid (DTPA) was prepared in 10 mM MOPS. A 50 mM $NaIO_4$ stock solution was prepared monthly in MQ. A 1 mM DAC working solution was prepared by adding 1 mM DA and 2mM $NaIO_4$ into buffer solutions containing 20 mM HCl before each experiment. Stock solution of 20 mM 2,2′-bipyridyl was prepared in 5 mM HCl. Ascorbate stock solution (200 mM) was prepared daily by dissolving L-ascorbic acid in 50 mM HCl. The Fe^{III}DFB complex used in this work was prepared by adding 0.5 mM

Fe(III) and 5 mM DFB into 10 mM HCl. Stock solutions of 1KU/ml tyrosinase was prepared in MQ water and stored in the freezer when not in use.

Measurement of DAC concentration

The concentration of DAC was quantified spectrophotometrically in a 10 cm cuvette by a Cary 60 spectrophotometer at 475 nm with baseline correction at 850 nm. [3, 4] Calibration curves were developed at different DAC concentrations are shown in Fig. S1. Briefly, in order to accelerate the cyclization rate of DAQ in the DAC working solution and prevent the faster decay of DAC at high pH, different concentrations of the freshly prepared DAC working solution was added into the buffer solutions at pH 7.0.

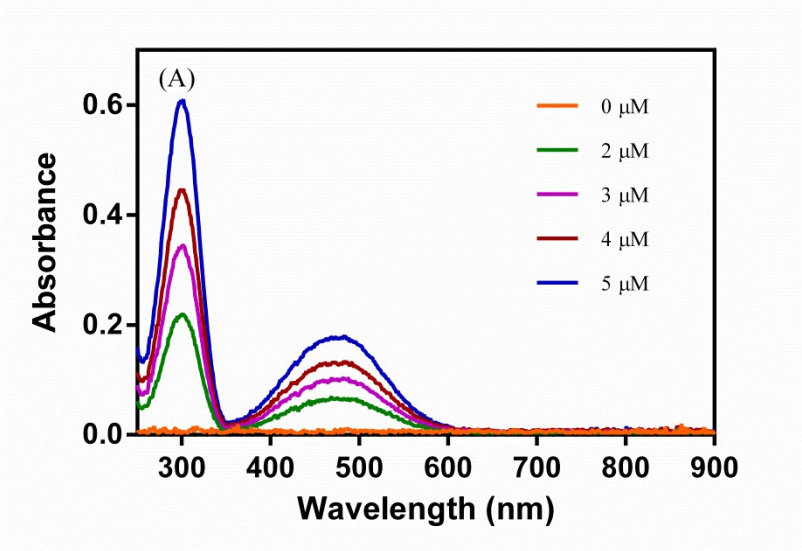

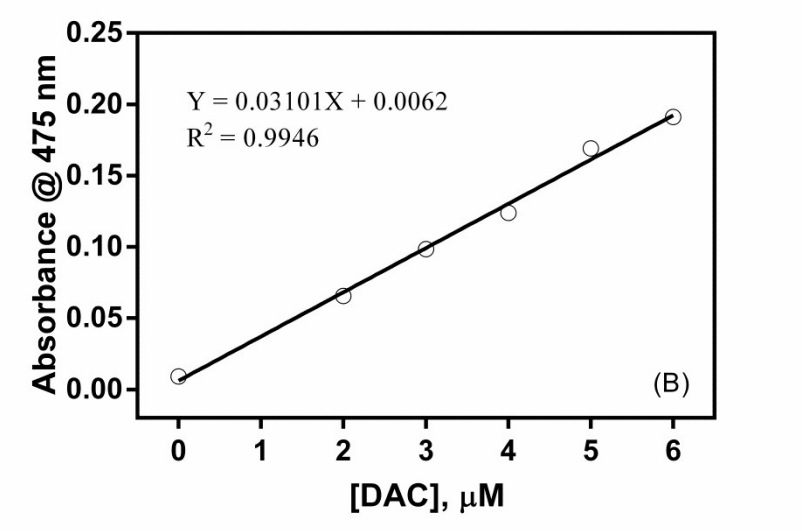

Figure S1. Measured absorbance of DAC (panel A) and calibration curve for qualification of DAC measured at 475 nm with baseline corrected at 850 nm (panel B) in 0.1 M NaCl.

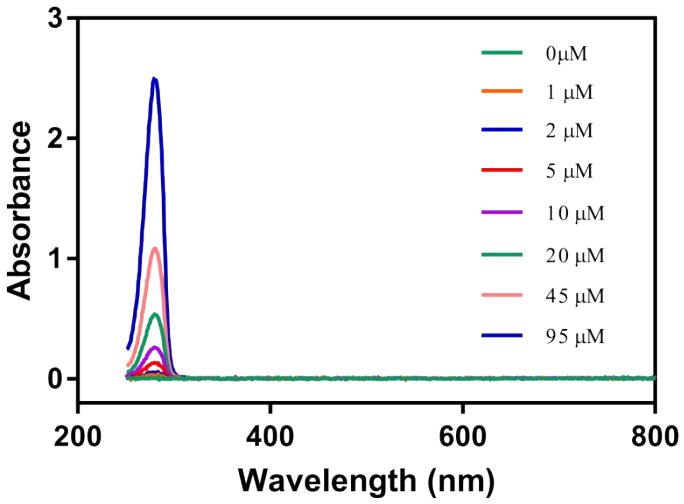

Figure S2. Measured absorbance of DA in 0.1 M NaCl

Measurement of H_2O_2 concentration

The H_2O_2 formed during the course of DA oxidation was quantified using the modified DPD method. [2, 5] 1 mM DTPA was added to halt the continuous generation of H_2O_2 during the measurement. [5] Considering the rapid oxidation of Fe(II) at pH 8.0, the influence of Fe(II) on the measurement of H_2O_2 is negligible during the timescale of the experiments. The system was calibrated by adding standard H_2O_2 stock into the buffer solutions, along with a zero standard containing 60 μM DPD and 500 U/L HRP.

SI 2 Speciation analysis

Stability constants for Fe(II) and Fe(III) speciations

Table S1. Stability constants for Fe(II) and Fe(III) speciations at 25 ℃ and Ionic Strength (*I*) = 0.

No.	species	Log*K*	Reference
Fe(II) species			
1	$Fe^{2+} + H_2O \rightleftharpoons FeOH^+ + H^+$	-9.51	Ref [6]
2	$Fe^{2+} + 2H_2O \rightleftharpoons Fe(OH)_2^0 + 2H^+$	-20.6	Ref [6]
3	$Fe^{2+} + CO_3^{2-} \rightleftharpoons FeCO_3^0$	5.69	Ref [7]
4	$Fe^{2+} + H^+ + CO_3^{2-} \rightleftharpoons FeHCO_3^+$	11.8	Ref [8]
5	$Fe^{2+} + 2CO_3^{2-} \rightleftharpoons Fe(CO_3)_2^{2-}$	7.45	Ref [7]
6	$Fe^{2+} + CO_3^{2-} + H_2O \rightleftharpoons Fe(OH)CO_3^- + H^+$	-4.03	Ref [7]
7	$Fe^{2+} + Cl^- \rightleftharpoons FeCl^+$	0.3	Ref [7]
8	$Fe^{2+} + SO_4^{2-} \rightleftharpoons FeSO_4^0$	2.42	Ref [7]
9	$Fe^{2+} + DA^{2-} \rightleftharpoons FeDA^0$	9.12	Ref [9]
10	$Fe^{2+} + 2DA^{2-} \rightleftharpoons FeDA_2^{2-}$	14.56	Ref [9]
Fe(III) species			
11	$Fe^{3+} + H_2O \rightleftharpoons Fe(OH)^{2+} + H^+$	-2.13	Ref [10]
12	$Fe^{3+} + 2H_2O \rightleftharpoons Fe(OH)_2^+ + 2H^+$	-6.13	Ref [10]
13	$Fe^{3+} + 3H_2O \rightleftharpoons Fe(OH)_3^0 + 3H^+$	-14.3	Ref [10]
14	$Fe^{3+} + 4H_2O \rightleftharpoons Fe(OH)_4^- + 4H^+$	-22.2	Ref [10]
15	$Fe^{3+} + Cl^- \rightleftharpoons FeCl^{2+}$	1.28	Ref [10]
16	$Fe^{3+} + 2Cl^- \rightleftharpoons FeCl_2^+$	1.16	Ref [10]
17	$Fe^{3+} + SO_4^{2-} \rightleftharpoons Fe(SO_4)^+$	4.27	Ref [10]
18	$Fe^{3+} + 2SO_4^{2-} \rightleftharpoons Fe(SO_4)_2^-$	6.11	Ref [10]
19	$Fe^{3+} + 2CO_3^{2-} \rightleftharpoons Fe(CO_3)_2^-$	19.6	Ref [10]
20	$Fe^{3+} + DA^{2-} \rightleftharpoons FeDA^+$	21.42	Ref [11]

21	$Fe^{3+} + 2DA^{2-} \rightleftharpoons FeDA_2^-$	36.46	Ref [11]
22	$Fe^{3+} + 3DA^{2-} \rightleftharpoons FeDA_3^{3-}$	45.08	Ref [11]
Aqueous species			
23	$H^+ + OH^- \rightleftharpoons H_2O$	14	Ref [12]
24	$H^+ + CO_3^{2-} \rightleftharpoons HCO_3^-$	10.3	Ref [12]
25	$2H^+ + CO_3^{2-} \rightleftharpoons H_2CO_3^*$	16.7	Ref [12]
26	$NH_3 + H^+ \rightleftharpoons NH_4^+$	9.24	Ref [6]
27	$H^+ + SO_4^{2-} \rightleftharpoons HSO_4^-$	1.99	Ref [6]
28	$Na^+ + CO_3^{2-} \rightleftharpoons NaCO_3^-$	1.27	Ref [7]
29	$Na^+ + H^+ + CO_3^{2-} \rightleftharpoons NaHCO_3^0$	10.1	Ref [7]
30	$Na^+ + SO_4^{2-} \rightleftharpoons NaSO_4^-$	1.06	Ref [7]
31	$NH_4^+ + SO_4^{2-} \rightleftharpoons NH_4SO_4^-$	1.03	Ref [13]
32	$H_2DA \rightleftharpoons HDA^- + H^+$	-10.58	Ref [4]
33	$HDA^- \rightleftharpoons DA^{2-} + H^+$	-12.07	Ref [4]

Distribution of main iron and DA species

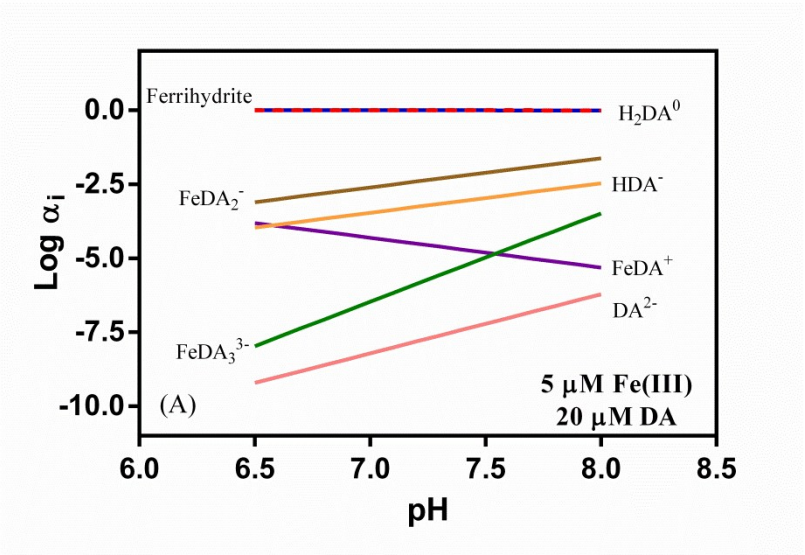

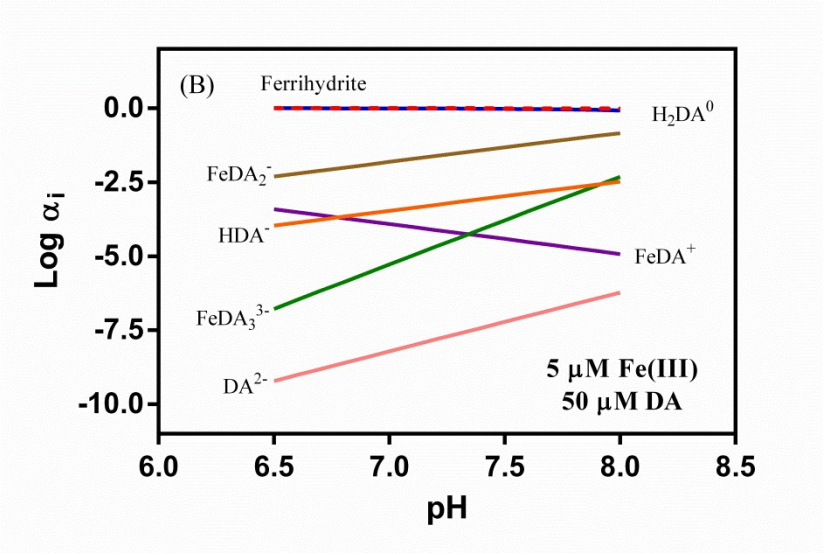

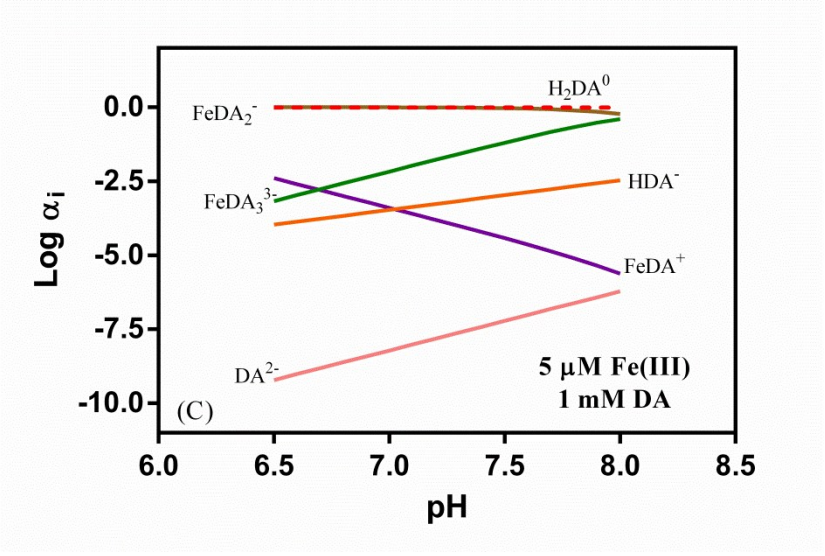

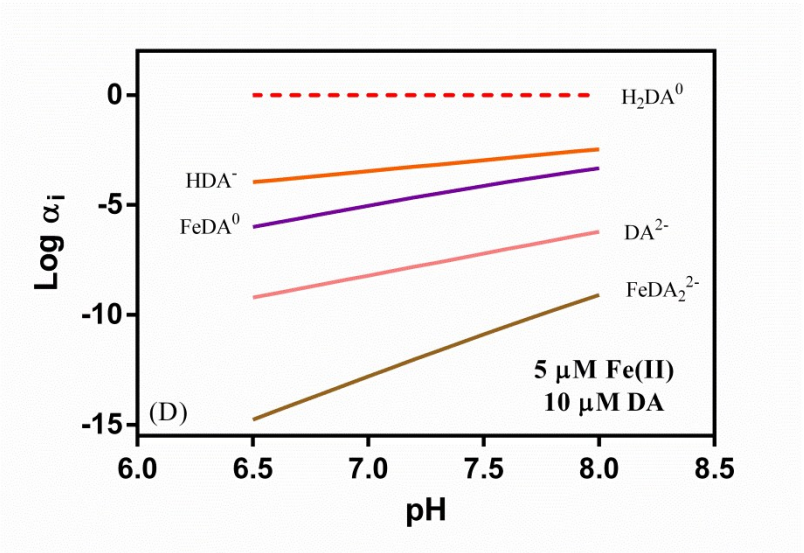

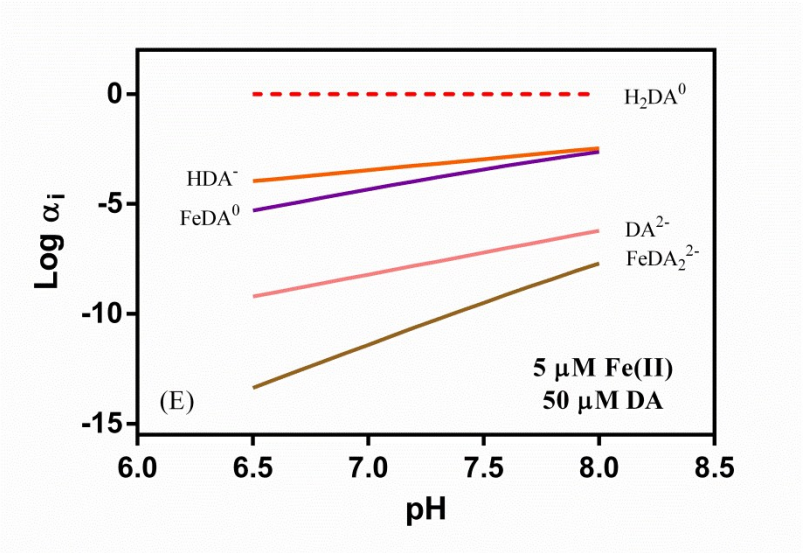

Figure S3. Distribution of different species of Fe(III) (A, B and C) and Fe(II) (D and E) over the pH range 6.5 - 8.0 in solutions containing varying concentrations of DA with $[Fe(III)]_0$ = 5 µM and $[Fe(II)]_0$ = 5 µM. αi denotes the molar fraction of individual species.

SI 3 Model justification

To assist the better understanding of the transformation of DA in the marine environment, a kinetic model was developed in this study by fitting to the experimental data at pH 8.0 over a range of conditions. All the rate constants used in the model fitting are summarized in Tables 1 - 3 in the main text. To better constrain the relatively complicated model developed in this study, several intermediates, including the formation of H_2O_2, DAC and DA bound iron, were measured. In general, an overall goodness of the model fitting to the experimental data indicates that the proposed mechanism should be reasonable. The relative importance of each reaction as well as the suitableness of the rate constant selected in this study is assessed by the sensitivity analysis. In specific, the more variation of the relative residuals to the change in the orders of magnitude in the rate constant, the more important the reaction is. The lowest point of the relative residual *r* generally represents the optimal value.

As shown in Fig. S4A, in accordance with the discussion in the main text, the oxidation of DA and its oxidative metabolites, DAL and DHI, is a critical process during the transformation of DA for the considerable sensitivity of the relative residual *r* to the change in the rate constant. Compared with the oxidation of DA and DAL, the rate constant proposed for the oxidation of DHI may only be a lower limit value for relative insensitivity above the proposed rate constant. As shown in Fig. S4B, in comparison with other radical reactions, the reduction of DAQ by $O_2^{\bullet-}$ is generally not important under oceanic condition since the relative residual *r* is not sensitive to the change in the rate constant over several orders of magnitude. The insensitivity of DAQ to $O_2^{\bullet-}$ under this condition may also indirectly confirm the negligible existence of DAQ as a result of its rapid cyclization. In general, the disproportionation of $DA^{\bullet-}$ is important in the transformation of DA in the marine environment as the relative residual *r* is sensitive to the change in the rate constant. The adopted rate constant for this reaction from previous work is reasonable since the value is consistent with the shift point obtained by the sensitivity analysis. As shown in Fig. S4C, compared with the rearrangement of DAC, the cyclization of DAQ and redox exchange between DAL and DAQ are generally not sensitive to the change in the rate constant. As such, the fitted rate constant for the cyclization process can only be treated as the lower limit values. The adopted rate constant for the redox exchange process [14] is generally

insensitive to values below the proposed one, which indicates that this value can only be an upper limit. The significant shift in the relative residual *r* to the change in rate constant indicates that the rearrangement of DAC is a critical process in the transformation of DA. The consistence of the proposed rate constant with the sensitive point indicates that the value proposed for this process is reasonable. Compared with the previous published rearrangement rate constant (3.3×10^{-4} ~ 10^{-3}/s) at pH 7.4, [15] the fitted rate constant (2.4×10^{-4}/s) in this study is reasonable.

As shown in Fig. S4D, in general, the interactions between ferric iron and DA are important processes for the sensitivity of these processes to the change in rate constant over several orders of magnitude. However, the rate constant proposed for the direct chelation of Fe(III) and replacement of the coordinated water can only be treat as the upper limit value for the relative insensitivity below the these values. Compared with previous study, [5] a much larger rate constant was proposed for the Fe(III) chelation herein. Theoretically, this is reasonable since the complexation process of DA is considerably favoured in the presence of *di*-anion. The increase in the content of *di*-anion on the increase in pH will give rise to an enhanced formation of the *mono*-complex. To minimize the number of the fitting parameter, the rate constant for the formation of the *bis*- and *tris*-complex from $Fe^{III}DA$ with another DA is assumed to be similar to the rate constant for water-loss from $Fe(OH)(H_2O)_5^{2+}$ of 4.50×10^5 $M^{-1}s^{-1}$. [16] In accordance with the argument in the main text, the smallest rate constant coupled with the clear shifting point of the iron mobilization process shown in Fig. S4D indicate this process should be one of the rate-limiting processes in the DA mediated iron transformation. As shown in Fig. S4E, while the dissociation of $Fe^{III}DA_3$ is important for the sensitivity of the relative residual *r* to the change in the rate constant, the rate constant proposed for this reaction should only be the lower limit as a result of the insensitivity greater than this value. The convergence of the proposed value with the shift point of the ligand exchange process indicates that the value proposed herein should be reasonable. As shown in Fig. S4F, the internal electron transfer between ferric iron and DA is important for the considerable sensitivity of the relative residual *r* to the change in the rate constants. The apparent decrease in the rate constant on the increase in the coordinated DA number is reasonable since it is widely recognized that the reactivity of the complexes is generally reduced on the increase in the occupation of the coordinated sites. Compared with previous study, [5] an enhanced rate constant for the reductive

dissolution was proposed in this work, which may arise from the pH induced enhancement in the reducing ability.

As shown in Fig. S4G, the considerable sensitivity of the relative residual *r* to the change in the rate constant of the complexation of Fe(II) by DA indicates that DA is critical in the transformation of Fe(II). Compared with previous study, [5] a considerable greater rate constant was proposed for the marine condition, which is reasonable since the enhanced deprotonation of DA at oceanic condition favours the complexation process. The oxidation of the so-formed $Fe^{II}DA$ complex can be significantly influenced by the presence of O_2, $O_2^{\bullet-}$ and $DA^{\bullet-}$ for the considerable sensitivity of the relative residual *r* to the change in the rate constant (Fig. S4G). However, except for the fitted value for O_2, the adopted rate constant from previous work at low pH range can only be treated as upper limit for the relative insensitivity of the relative residual below the rate constant used herein.

In general, $O_2^{\bullet-}$ is important both in the transformation of oxidant and reductant. As shown in Fig. S4H, the adopted values from previous work for the disproportionation of $O_2^{\bullet-}$ and $O_2^{\bullet-}$ induced reduction of amorphous ferric oxyhydroxide (ferrihydrite, AFO) can only be treated as the upper limits for the relative insensitivity of the relative residual *r* below the rate constant used herein. In contrast, the oxidation of $DA^{\bullet-}$ by $O_2^{\bullet-}$ is an important sink for these two radicals for the great sensitivity of the relative residual, especially in view of H_2O_2 generation. The convergence of the shift point with the adopted rate constant indicates that the previous proposed value is reasonable.

To simplify the complicated model, despite being considered to be important at low pH range, several reactions is omitted under oceanic condition for the insensitivity to the change in the rate constant both shown in the sensitivity analysis and the Kintek Explorer program. As shown in Fig. S4I, the interaction between Fe(III) and Fe(II) with $DA^{\bullet-}$ as well as $Fe^{II}DA$ and $Fe^{III}DA$ with $O_2^{\bullet-}$ is not sensitive to change around the previous proposed values. The underpinning reason for the insensitivity may arise from the generally low concentrations of the reactants. Specifically, under the marine condition, the ferric and ferrous iron mainly exist as the AFO or the organics bound iron with resultant the concentration of the free inorganic bound iron being rarely existed. As such, the interaction

between $DA^{\bullet-}$ with Fe(III) and Fe(II) should be not important. In view of $O_2^{\bullet-}$, as discussed above, the interaction between $DA^{\bullet-}$ and $O_2^{\bullet-}$ should be a major sink of $O_2^{\bullet-}$. Therefore, the significant oxidation of $Fe^{II}DA$ by O_2 under marine condition coupled with relative non-available of $O_2^{\bullet-}$ should render the interaction between these two species less important. In a manner similar to the case of $Fe^{II}DA$, the rapid formation of the *bis*- and *tris*-complexes coupled with relative non-available of $O_2^{\bullet-}$ should render the interaction between $Fe^{III}DA$ and $O_2^{\bullet-}$ less important.

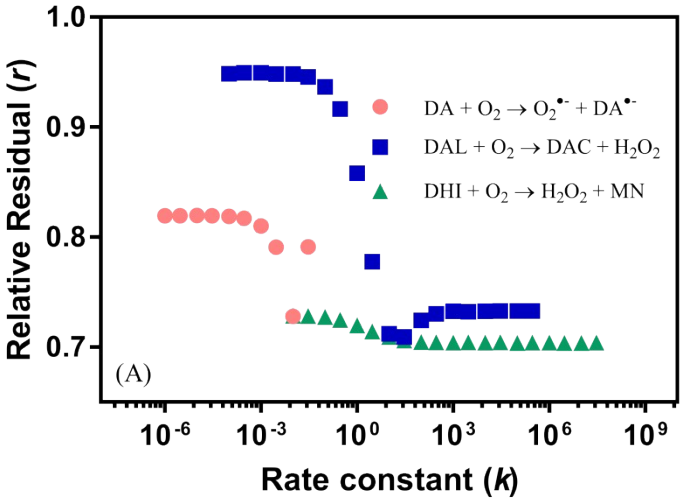

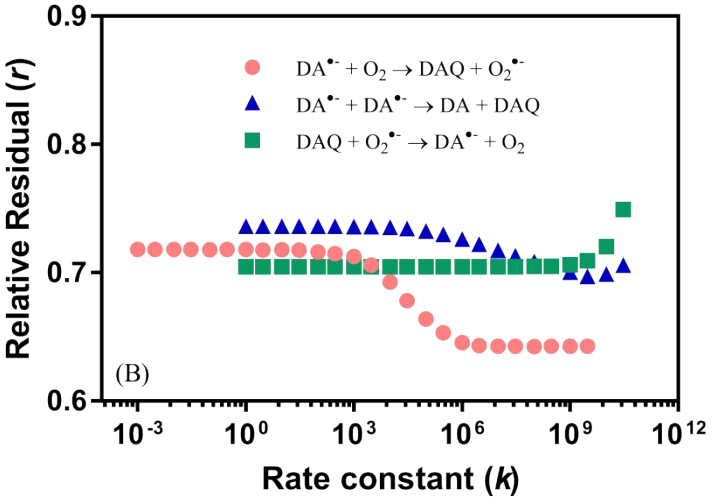

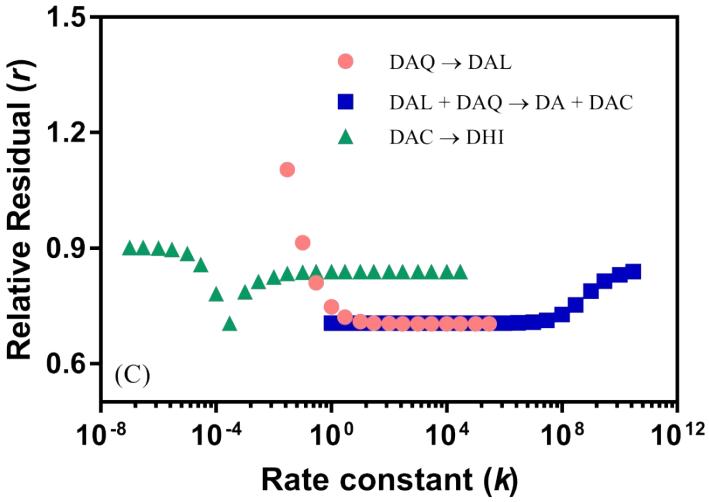
1.5
1.2
0.9
0.6
Relative Residual (r)
DAQ → DAL
DAL + DAQ → DA + DAC
DAC → DHI
(C)
10-8
10-4
100
104
108
1012
Rate constant (k)

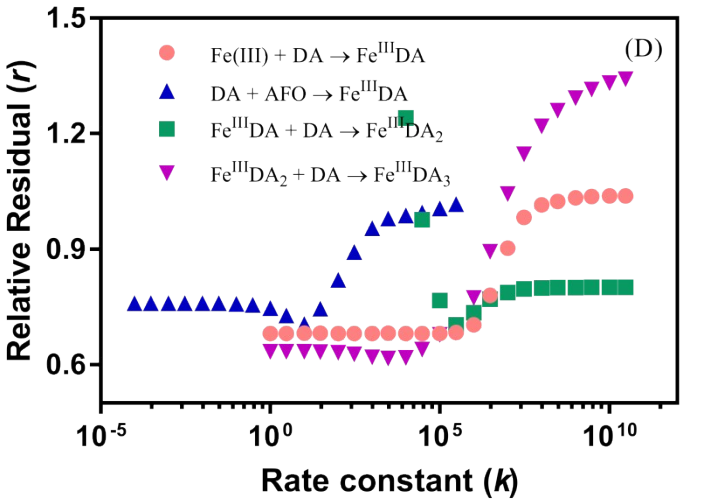
1.5
1.2
0.9
0.6
Relative Residual (r)
Fe(III) + DA → FeIIIDA
DA + AFO → FeIIIDA
FeIIIDA + DA → FeIIIDA2
FeIIIDA2 + DA → FeIIIDA3
(D)
10-5
100
105
1010
Rate constant (k)

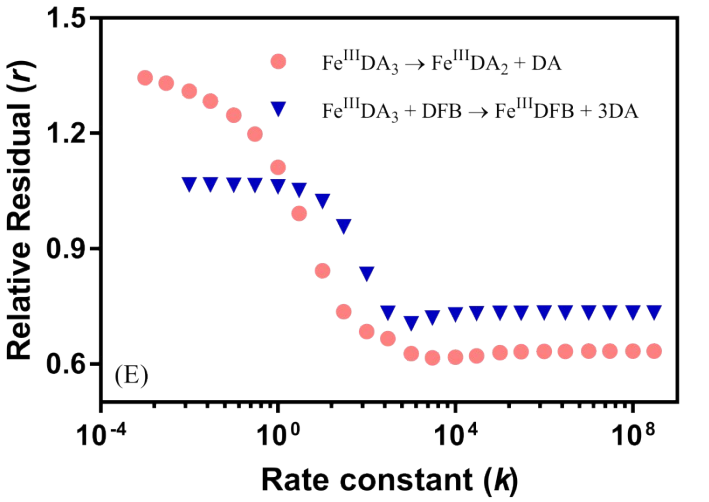
1.5
1.2
0.9
0.6
Relative Residual (r)
FeIIIDA3 → FeIIIDA2 + DA
FeIIIDA3 + DFB → FeIIIDFB + 3DA
(E)
10-4
100
104
108
Rate constant (k)

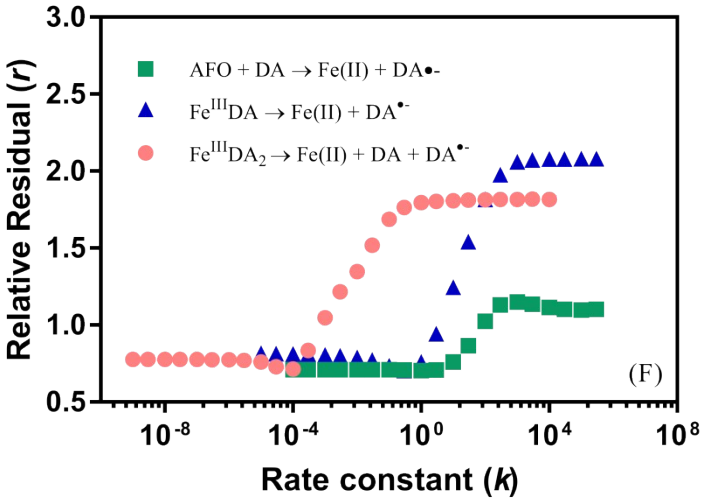
Relative Residual (r)
3.0
2.5
2.0
1.5
1.0
0.5
AFO + DA → Fe(II) + DA•-
Fe^III DA → Fe(II) + DA•-
Fe^III DA2 → Fe(II) + DA + DA•-
(F)
10^-8
10^-4
10^0
10^4
10^8
Rate constant (k)

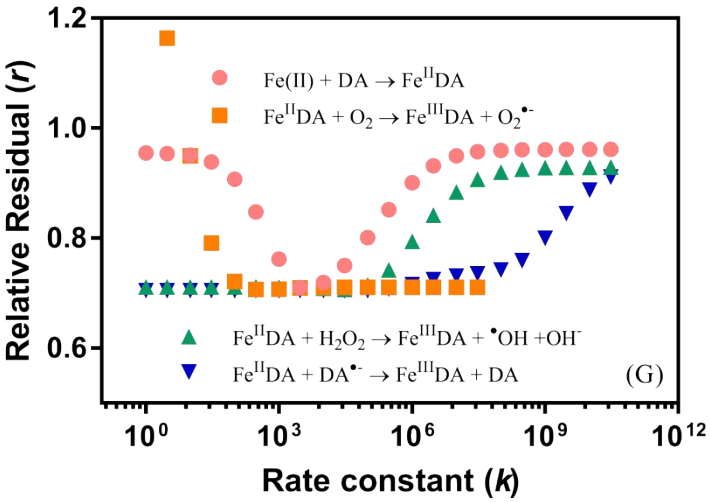
Relative Residual (r)
1.2
1.0
0.8
0.6
Fe(II) + DA → Fe^II DA
Fe^II DA + O2 → Fe^III DA + O2•-
Fe^II DA + H2O2 → Fe^III DA + •OH +OH-
Fe^II DA + DA•- → Fe^III DA + DA
(G)
10^0
10^3
10^6
10^9
10^12
Rate constant (k)

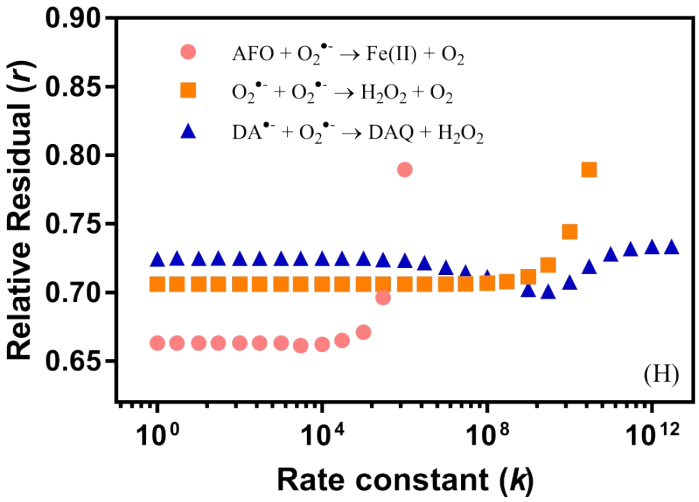
Relative Residual (r)
0.90
0.85
0.80
0.75
0.70
0.65
AFO + O2•- → Fe(II) + O2
O2•- + O2•- → H2O2 + O2
DA•- + O2•- → DAQ + H2O2
(H)
10^0
10^4
10^8
10^12
Rate constant (k)

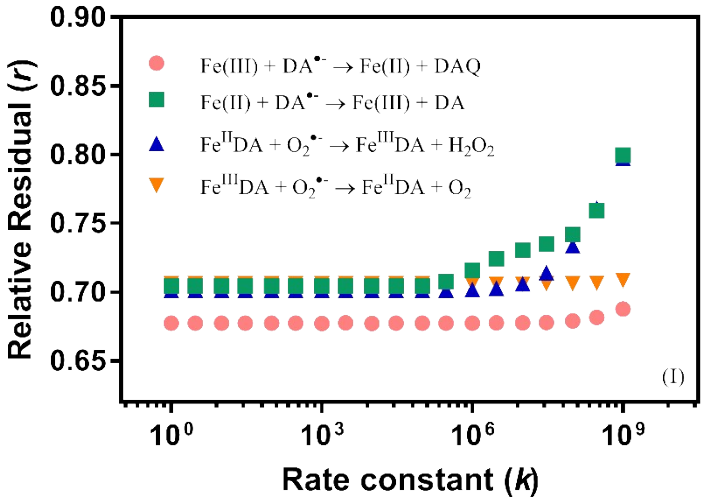

Figure S4. Sensitivity analysis for the fitted rate constants of different reactions (Tables 1-3, main text).

SI 4 Supplementary results

Spectrum of DA o-quinone (DAQ)

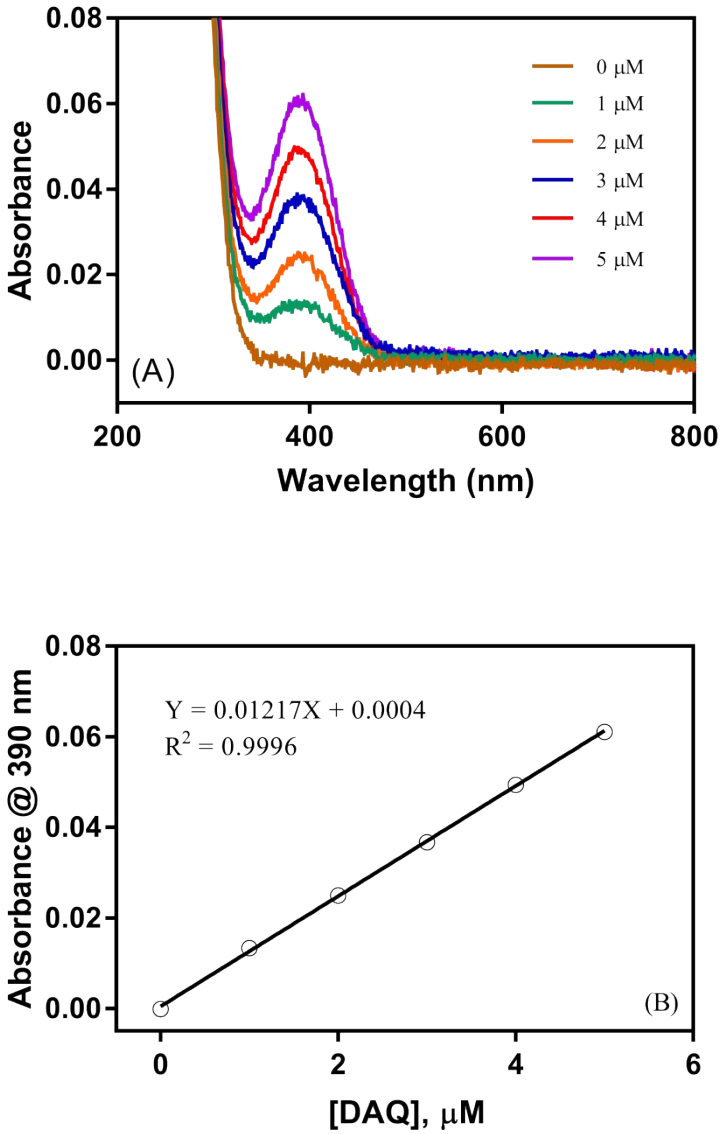

Figure S5. Measured absorbance of DAQ (panel A) and calibration curve for qualification of DAQ measured at 390 nm with baseline correction at 690 nm (panel B) in 0.1 M NaCl at pH 8.0.

The calibration curves of DAQ were conducted by adding different DAC working solutions into buffer solutions at pH 1.5. The calculated molar absorptivity of DAQ in this study is close to the previous reported value (1,330 $M^{-1}cm^{-1}$). [17] The reason that DAC working solutions can be used in the calibration of DAQ is that, as a result of the extremely

acidic condition of the working solution, the substance actually present is DAQ. At pH 1.5, the cyclization of DAQ is negligible. In contrast, the instantaneous cyclization of DAQ at pH 7.0 results in all the DAQ present in the solution being converted into DAC with this evident from the reasonable molar absorptivity derived from the calibration curves.

Formation of melanin form the decay of DAC

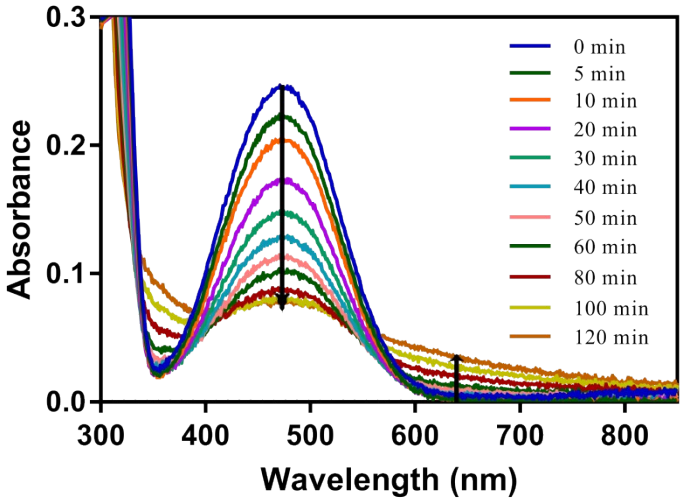

Figure S6. Decay of 8 µM DAC at pH 8.0 in the presence of 0.1 M NaCl, 10 mM MOPS and 2 mM $NaHCO_3$.

As shown in Fig. S6, the decay of DAC is accompanied by the increase in the background of the spectrum overtime, which generally arises from the polymerization of the intermediates and the concomitant formation of melanin.

Predicted Concentration of DAQ

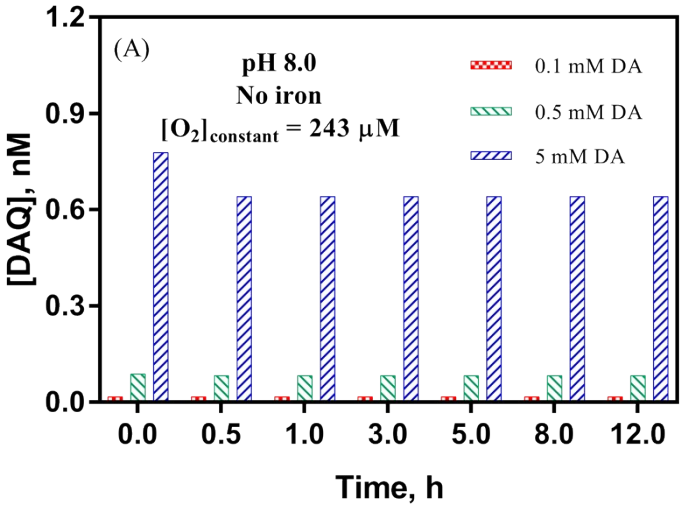

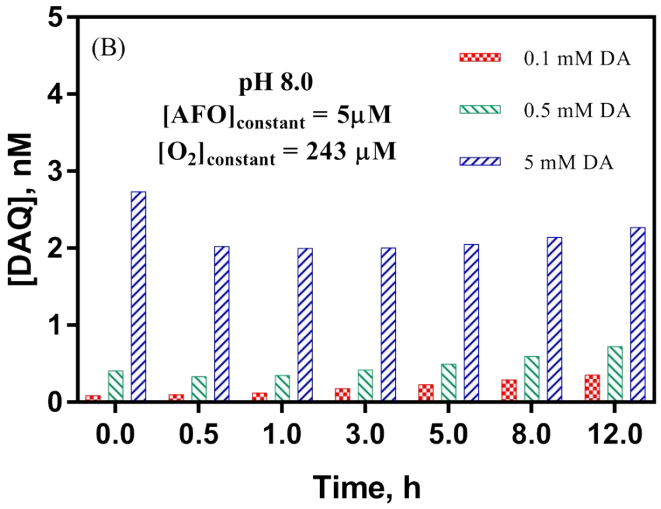

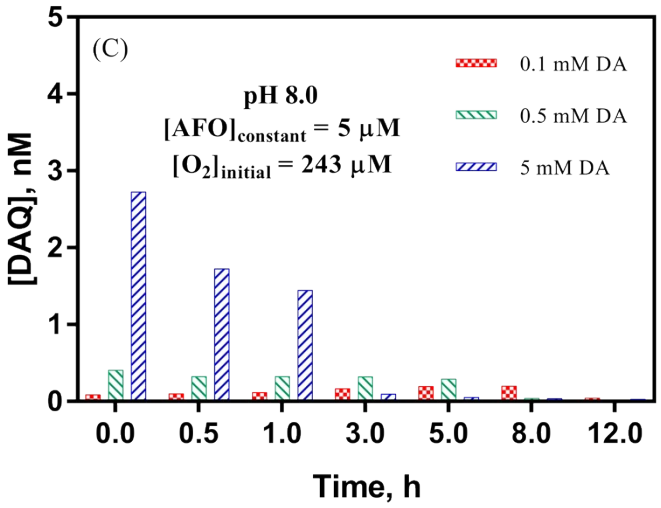

Figure. S7 Predicted concentrations of DAQ generated in air-saturated buffer solutions with fixed concentrations of DA and O_2 (panel A), fixed concentrations of O_2, DA and AFO (panel B) and fixed concentrations of DA and AFO (panel C).

Formation of melanin in synthetic seawater

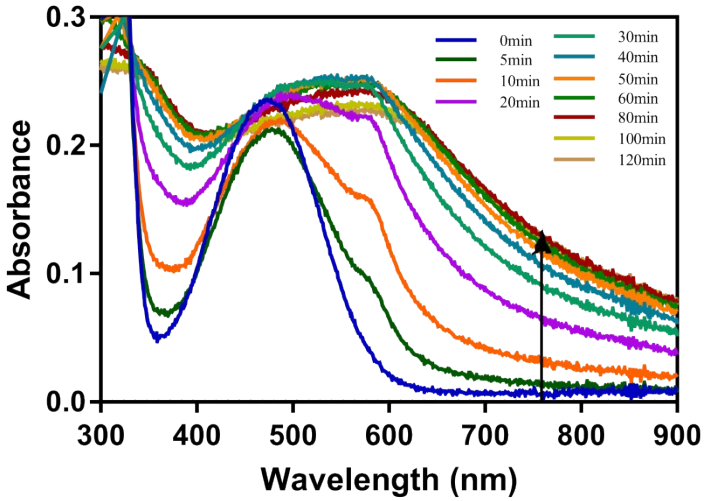

Figure S8. Spectrum of decay of pure DAC in synthetic seawater at pH 8.0.

Effect of DA on the transformation of Fe(II)

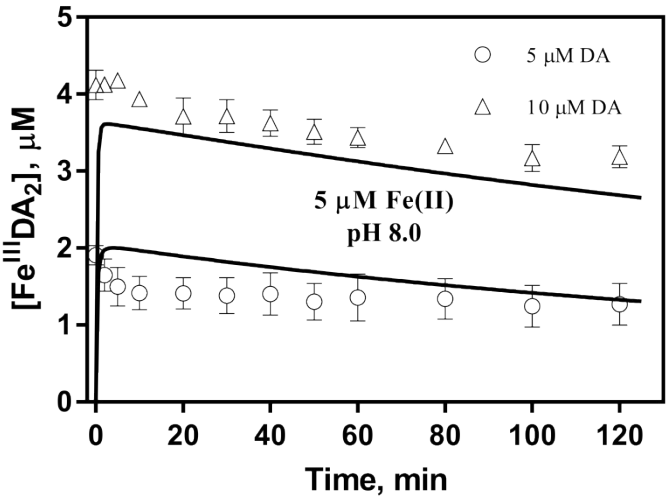

Figure S9. Formation of $Fe^{III}DA_2$ complex on addition of 5 μM Fe(II) into (○) 5 μM DA and (Δ) 10 μM DA at pH 8.0 in 0.1 M NaCl. Error bars are standard errors from triplicate measurements and solid lines represent the model fit.

Effect of the oxidation of DHI on the generation of H_2O_2

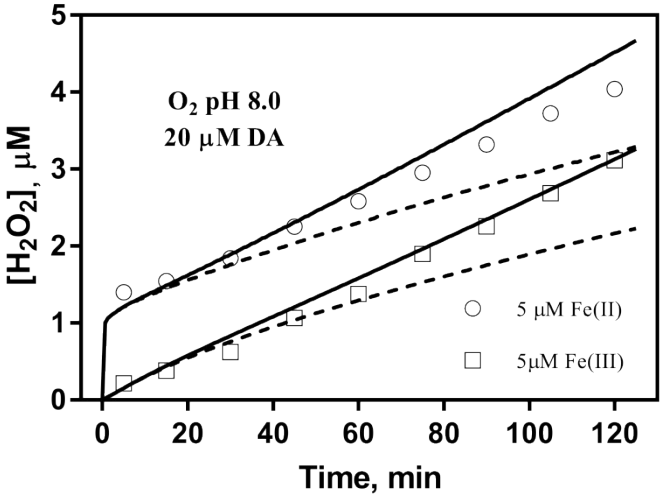

Figure S10. Formation of H_2O_2 in 20 μM DA containing 0.1 M NaCl solutions in the presence of (○) 5 μM Fe(II) and (□) 5 μM Fe(III) at pH 8.0. The solid lines represent the model fitting involving the oxidation of DHI and the dashed lines represent the model prediction without the oxidation of DHI.

Absorbance of DA bound Ca^{2+} and Mg^{2+}

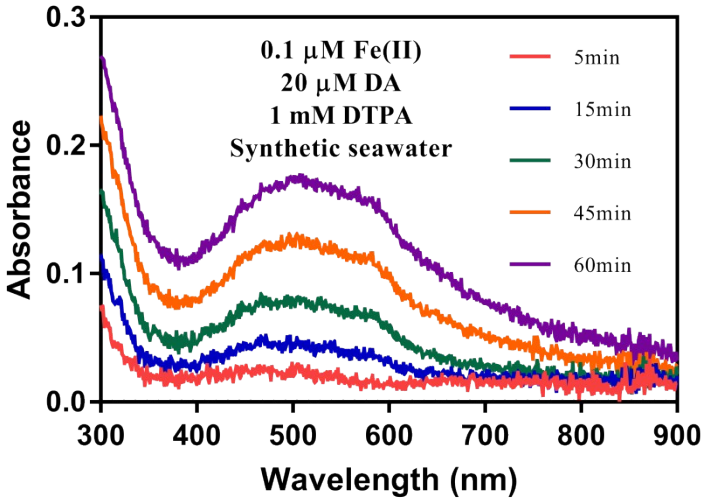

Figure S11. Formation of DA bound Ca^{2+} or Mg^{2+} in synthetic seawater containing 0.1 µM Fe(II), 20 µM DA and 1 mM DTPA.

Effect of Tyrosinase on the oxidative transformation of DA

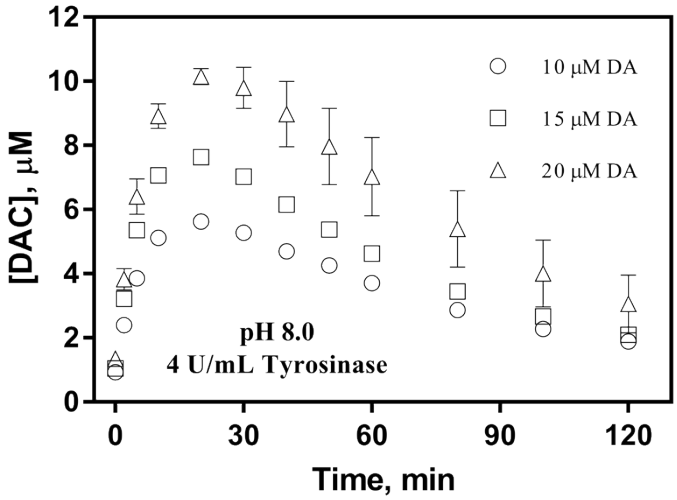

Figure S12. Effect of Tyrosinase on the oxidative transformation of DA in buffer solutions at pH 8.0.

Transformation of $Fe^{III}DA_3$ over time

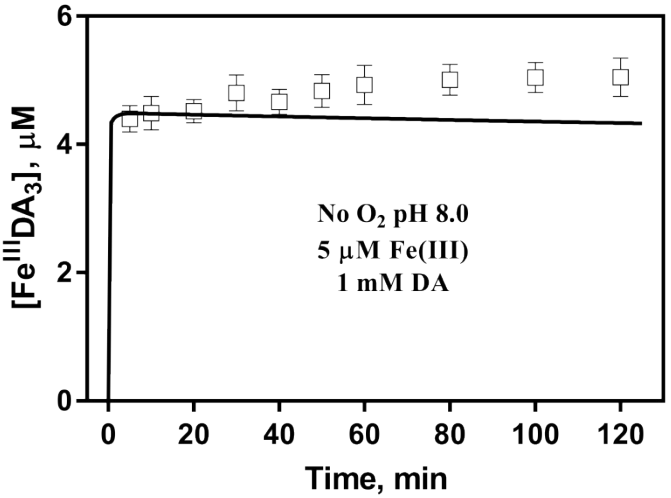

Figure S13. Formation and transformation of $Fe^{III}DA_3$ over time at pH 8.0 in 0.1 M NaCl. Error bars are standard errors from triplicate measurements and solid lines represent the model fit.

SI 5 Equilibrium calculation for the Fe-DA complexes

Generally, all the forms of DA (including H_2DA^0, HDA^- and DA^{2-}) can form complexes with iron. The stability constants listed in Table S1 is the one between iron and DA^{2-}. In the presence of H_2DA^0 or HDA^-, the associated stability constant for the equilibrium would change accordingly for the participation of H^+. An example is shown below for the calculation of stability constant between Fe(III) and H_2DA^0.

For the equilibrium between $Fe^{3+} + H_2DA^0 \leftrightarrow FeDA^+ + 2H^+$, the stability constant K^* can be written as follows:

$$K^* = \frac{[FeDA^+][H^+]^2}{[Fe^{3+}][H_2DA^0]} = \frac{[FeDA^+]}{[Fe^{3+}][DA^{2-}]} \times \frac{[DA^{2-}][H^+]^2}{[H_2DA^0]} = K \times K_{a1} \times K_{a2} \qquad \text{Eq (S1)}$$

As such, LogK^* can be calculated as -2.64 by using the stability constant listed in Table S1. The definition of stability constant is

$$K = \frac{k_+}{k_-} \qquad \text{Eq (S2)}$$

where k_+ and k_- are the associated formation and dissociation rate constant. [6] Thus, for a given formation rate constant, the corresponding dissociation rate constant can be calculated as k_+/K. Even though H_2DA^0 is the dominant DA species over the pH range investigated in this study, increase in much more active HDA^- as well as DA^{2-} with increase in pH would definitely decrease the apparent dissociation rate constant.

Reference

1. Morgan, M. S.; Van Trieste, P. F.; Garlick, S. M.; Mahon, M. J.; Smith, A. L., Ultraviolet molar absorptivities of aqueous hydrogen peroxide and hydroperoxyl ion. *Anal. Chim. Acta* **1988,** *215*, 325-329.

2. Bader, H.; Sturzenegger, V.; Hoigne, J., Photometric method for the determination of low concentrations of hydrogen peroxide by the peroxidase catalyzed oxidation of N, N-diethyl-*p*-phenylenediamine (DPD). *Water Res.* **1988,** *22*, (9), 1109-1115.

3. Herlinger, E.; Jameson, R. F.; Linert, W., Spontaneous autoxidation of dopamine. *J. Chem. Soc., Perkin Trans. 2* **1995**, (2), 259-263.

4. Pham, A. N.; Waite, T. D., Cu (II)-catalyzed oxidation of dopamine in aqueous solutions: Mechanism and kinetics. *J. Inorg. Biochem.* **2014,** *137*, 74-84.

5. Sun, Y.; Pham, A. N.; Waite, T. D., Elucidation of the interplay between Fe (II), Fe (III), and dopamine with relevance to iron solubilization and reactive oxygen species generation by catecholamines. *J. Neurochem.* **2016,** *137*, (6), 955-968.

6. Morel, F. M.; Hering, J. G., *Principles and applications of aquatic chemistry*. Wiley: New York, 1993.

7. King, D. W., Role of carbonate speciation on the oxidation rate of Fe (II) in aquatic systems. *Environ. Sci. Technol.* **1998,** *32*, (19), 2997-3003.

8. Millero, F. J.; Hawke, D. J., Ionic interactions of divalent metals in natural waters. *Mar. Chem.* **1992,** *40*, (1), 19-48.

9. Smith, R. M.; Martell, A. E., *Critical stability constants, Vol. 6: Second Supplement*. Plenum Press: New York, USA, 1989; Vol. 6.

10. Pham, A. N.; Rose, A. L.; Feitz, A. J.; Waite, T. D., Kinetics of Fe(III) precipitation in aqueous solutions at pH 6.0–9.5 and 25°C. *Geochim. Cosmochim. Acta* **2006,** *70*, (3), 640-650.

11. Avdeef, A.; Sofen, S. R.; Bregante, T. L.; Raymond, K. N., Coordination chemistry of microbial iron transport compounds. 9. Stability constants for catechol models of enterobactin. *J. Am. Chem. Soc.* **1978,** *100*, (17), 5362-5370.

12. Millero, F. J.; Yao, W.; Aicher, J., The speciation of Fe (II) and Fe (III) in natural waters. *Mar. Chem.* **1995,** *50*, (1), 21-39.

13. Schecher, W. D.; McAvoy, D. C., MINEQL+: a software environment for chemical equilibrium modeling. *Comput. Environ. Urban Syst.* **1992,** *16*, (1), 65-76.

14. Land, E.; Ito, S.; Wakamatsu, K.; Riley, P., Rate constants for the first two chemical steps of eumelanogenesis. *Pigm. Cell Res.* **2003,** *16*, (5), 487-493.

15. Bisaglia, M.; Soriano, M. E.; Arduini, I.; Mammi, S.; Bubacco, L., Molecular characterization of dopamine-derived quinones reactivity toward NADH and glutathione: implications for mitochondrial dysfunction in Parkinson disease. *Biochim. Biophys. Acta, Mol. Basis. Dis.* **2010,** *1802*, (9), 699-706.

16. Blesa, M. A.; Matijević, E., Phase transformations of iron oxides, oxohydroxides, and hydrous oxides in aqueous media. *Adv. Colloid Interfac* **1989,** *29*, (3), 173-221.

17. Waite, J. H., Calculating extinction coefficients for enzymatically produced *o*-quinones. *Anal. Biochem.* **1976,** *75*, (1), 211-218.